NATURALISTIC MUSIC STABILIZES ALPHA-BAND PHASE DYNAMICS IN HUMAN ELECTROENCEPHALOGRAM

Anonymous authors
Paper under double-blind review

ABSTRACT

The temporal evolution of neuronal phase and its predictability in naturalistic settings, such as music listening, remains underexplored in the alpha-band (8-13 Hz) of electroencephalogram (EEG) studies. In this study, we propose a novel framework for quantifying short-horizon phase predictability and phase stability by modeling phase prediction errors using a linear approximation that captures the diffusion-like behavior of alpha-band oscillations. The framework was evaluated on two music-EEG datasets. The first dataset consists of EEG data from 13 healthy participants listening to live Indian classical music (ICM), comprising two ragas and relaxation conditions. The second dataset, the naturalistic music EEG dataset - tempo (NMED-T), consisted of EEG recordings from 20 participants listening to 10 songs. For both datasets, individual alpha frequencies (IAF) were computed to obtain subject-specific band-pass signals. Instantaneous phase was extracted from the analytic signal using the Hilbert transform and predicted over short horizons ($\Delta = 50, 100, 150, 200$ ms) using instantaneous frequency estimates. Mean absolute phase prediction errors were modeled linearly to estimate the diffusion slope, providing a measure of phase stability. The results from the ICM dataset showed consistently higher phase prediction errors during the relaxation condition than during both music conditions. The diffusion slopes were lower during music, suggesting slower accumulation of phase prediction error and greater short-horizon phase stability. Paired t-tests revealed statistically significant differences between music and relaxation for both phase prediction errors and diffusion slopes. Comparative results were observed on the NMED-T dataset. These findings demonstrate that naturalistic music listening is associated with more stable alpha-band phase dynamics, providing a quantitative framework for assessing neural oscillatory stability in continuous EEG signals.

1 INTRODUCTION

Neural oscillations are a fundamental mechanism for coordinating brain activity across spatial and temporal scales, enabling large scale integration and communication between cortical regions. Neural oscillations encompass multiple frequency bands, each associated with distinct functional roles in cognition and behavior, reflecting a hierarchical organization of brain dynamics across temporal scales Buzsáki (2006); Niedermeyer & da Silva (2005); Mantini et al. (2007). Among these, alpha-band oscillations (8-13 Hz) have been extensively studied and are known to play a key role in attention, memory, and sensory processing Klimesch (1999); Klimesch et al. (1997); Nunez & Srinivasan (2006); Cruz et al. (2025); Palva & Palva (2007); Foxe & Snyder (2011). Variations in alpha activity have been linked to changes in cortical excitability, with increased alpha power often associated with functional inhibition and reduced processing of irrelevant sensory inputs Klimesch et al. (2007); Jensen & Mazaheri (2010); Malekmohammadi et al. (2023); Mizokuchi et al. (2024). This inhibitory role of alpha-band oscillations provides a critical mechanism for regulating information flow in the brain during cognitive and perceptual tasks. Electroencephalogram (EEG) studies have indicated systematic variations of alpha-band activity related to cognitive engagement and emotional processing during music listening Lin et al. (2010); Sammler et al. (2007). The structure of music (rhythm and melody) influences the ongoing neural oscillations. This indicates a close relationship

Reviewers: please read the Reviewer Guidelines (iclr.cc/Conferences/2027/ReviewerGuidelines) and the AI Policy for Reviewers (iclr.cc/Conferences/2027/AIPolicyForReviewers). If you used AI to expand, edit, or polish your review, please provide the input text to the LLM. Better still, consider skipping the LLM and submitting your original text: we, and the authors, are much more interested in your unedited thoughts than in what an LLM has to say. AI-assisted or not, you are putting your name and reputation behind your review: LLM-generated falsehoods, hallucinations or misrepresentations are subject to disciplinary action, which may include desk-rejecting all papers you have authored.

between auditory stimuli and brain dynamics Nozaradan et al. (2011); Large et al. (2015); Tichko et al. (2022); Spiech et al. (2024); Kaneshiro et al. (2024). However, most of these previous studies have focused on spectral power Pascucci et al. (2025), highlighting amplitude-based measures of neural activity and providing limited insight into the temporal dynamics of oscillatory phase.

Beyond amplitude-based measures, the phase of neural oscillations plays an important role in determining the timing of neuronal excitability and communication between brain regions Fries (2005); Siegel et al. (2012). Phase-based measures such as phase-locking value (PLV) and inter-trial phase coherence (ITPC) are commonly used to quantify synchronization between trials and brain regions Lachaux et al. (1999); Delorme & Makeig (2004); Cohen (2014). Although these measures have provided valuable insights into stimulus-driven synchronization and large-scale neural coordination, they are fundamentally dependent on trial structure and external temporal alignment. As a result, they are challenging for continuous and naturalistic recordings Sonkusare et al. (2019); Hasson et al. (2004), where neural dynamics evolve without explicit temporal alignment. Addressing such data requires methods that can track the effective evolution of phase over time. Naturalistic EEG recordings obtained during tasks such as music listening or real-world cognition are non-stationary and lack well-defined temporal alignment. Under these conditions, neural oscillations are more appropriately characterized as continuously evolving stochastic processes than as event-locked responses. Their analysis requires frameworks that capture the ongoing evolution of the oscillatory phase, rather than approaches that rely on synchronization events. Such frameworks should characterize not only instantaneous phase variation but also the temporal persistence and predictability of the underlying oscillatory process. Neural oscillations, when analyzed from a dynamical systems perspective, are often represented as noisy limit-cycle systems where phase evolves due to both deterministic dynamics and stochastic perturbations Pikovsky et al. (2003); Kuramoto (1984); Nakao (2016). The phase variability of these systems accumulates over time in a diffusion-like manner, resulting in a loss of phase predictability Nakao (2016). This phenomenon, termed phase diffusion, has been extensively studied in nonlinear dynamical systems and serves as a systematic framework for analyzing the stability of oscillatory processes Winfree (1980); Ermentrout & Terman (2010). Although phase diffusion is well established in nonlinear dynamical systems, its empirical characterization in continuous EEG recordings remains limited.

Although previous studies have primarily relied on trial-based and amplitude-based measures, less is known about the short-term evolution of the phase of alpha-band oscillations during continuous naturalistic conditions. Examining the local predictability of alpha-band phase offers a way to quantify the stability of ongoing neural oscillations beyond conventional synchronization measures. The accumulation of phase deviations over short time scales can then be used to assess whether the underlying dynamics exhibit diffusion-like behavior. In this study, we evaluate how structured auditory stimuli, such as music, influence oscillatory stability. More broadly, this perspective extends the analysis of continuous EEG recordings in naturalistic settings by linking concepts from stochastic oscillator theory to empirical measures of phase stability. To the best of our knowledge, this is among the first studies to investigate short-horizon phase predictability and diffusion-like alpha-band dynamics in continuous EEG recordings during naturalistic music listening.

The key contributions of this manuscript are as follows:

- A novel framework is proposed for quantifying short-horizon phase predictability in alpha-band continuous EEG signals.
- Diffusion-like phase dynamics are characterized by modeling the growth of phase prediction error across multiple temporal horizons using a linear diffusion slope measure.

2 Dataset, and volunteers

2.1 Dataset

For this study, we used a dataset in which participants' EEG signals were recorded while they listened to live vocal Indian classical music (ICM). The data was collected using a structured musical paradigm using two ragas: Yaman and Puriya Dhanashree (PD). Further details regarding the music paradigm can be found in these studies Shivakumar et al. (2026b;a); Panda et al. (2024; 2023). The structure of the musical paradigm is presented below:

Initiation: 30-45 sec
Raga Yaman: 3 min
Relaxation: 2 min
Transition: 2 min
Raga Puriya Dhanashree (PD): 3 min
Relaxation: 2 min

The music paradigm starts with an initiation of 30-45 seconds duration. Both ragas (Yaman and Puriya Dhanashree) are 3 minutes long, and both relaxation conditions are 2 minutes long. During relaxation periods, no music is played, but the EEG is recorded. In the transition condition, Raga Yaman is played for the first one minute, then gradually transitions into Raga Puriya Dhanashree. The exact timestamps for each condition vary across participants, as live music is used in the paradigm. While listening to music, the participants closed their eyes.

2.2 PARTICIPANTS

A total of 13 healthy volunteers were recruited for this study, including 11 males and 2 females. Four participants had prior knowledge of classical music, while the remaining had no prior knowledge. The mean age of the participants is 30.54 ± 9.42 years. The summary of the demographic details are presented in Table 1. None of the participants reported a history of neurological disorders and hearing impairments. All participants were informed about the experimental procedure prior to data collection. The study protocol was approved by the Institutional Ethics Committee. All the volunteers provided written consent prior to the data collection.

Table 1: Summary of participants involved in the study.

Characteristic	**Value**
Total participants	13
Male	11
Female	2
Age range (years)	21-52
Participants with prior music knowledge	4
Participants without prior music knowledge	9

EEG data were collected using a 24-channel electrode cap (EASYCAP (RBE-24-STD)). Prior to data recording, the scalp was cleaned with alcohol, and conductive gel was applied to ensure low electrode impedances. The impedances were maintained in the range 10-20 kΩ. The electrodes were positioned according to the standard 10-20 system H. (1958). Data acquisition was performed using the CameraEEG smartphone application Hazarika et al. (2023), with a sampling frequency of 500 Hz.

3 METHODOLOGY

This section describes the proposed framework for quantifying short-horizon phase predictability and estimating phase diffusion in alpha-band EEG activity. The pipeline comprises four sequential stages: (a). EEG preprocessing and channel selection, (b). Estimation of the individual alpha frequency (IAF), (c). Phase estimation and short-horizon prediction, and (d). Diffusion slope estimation.

3.1 PREPROCESSING AND CHANNEL SELECTION

EEG data were recorded at a sampling rate of 500 Hz. Faulty channels were identified through visual inspection and excluded from the study. Artifact correction was then performed using the MATLAB toolbox described in Somers et al. (2018) to remove eye blinks, muscle, and movement artefacts. All subsequent analyses were conducted on the resulting clean EEG data. In this study, the two relaxation conditions were concatenated into a single condition for subsequent analysis.

Alpha-band oscillations are predominantly expressed in posterior cortical regions Klimesch (1999); Nunez & Srinivasan (2006). Accordingly, a subset of posterior electrodes (O1, O2, POz, and Pz)

was selected for subsequent analysis. For each subject, the signals from the selected channels were denoted as $X_k(t)$, where k indexes the channel and t denotes time samples. Let K be the number of retained posterior channels after artefact rejection and faulty channel removal. To obtain a robust representation of posterior alpha-band activity, a spatial average across the chosen channels was computed as:

$$x(t) = \frac{1}{K} \sum_{k=1}^{K} X_k(t) \tag{1}$$

The resulting signal $x(t)$ in Eq. 1 represents the mean posterior time series and serves as the basis for subsequent analysis. This averaging step improves signal-to-noise ratio (SNR) and emphasizes spatially coherent alpha activity.

3.2 Individual alpha frequency (IAF) estimation

Alpha oscillations exhibit substantial inter-individual variability in peak frequency, commonly referred to as the individual alpha frequency (IAF), which has been linked to cognitive processing and neural efficiency Grandy et al. (2013). The power spectral density (PSD) of the mean posterior signal $x(t)$ was estimated using Welch's method. $P(f)$ denotes the resulting PSD as a function of frequency f. The individual alpha frequency (IAF) was defined as the frequency corresponding to the maximum power within the alpha band (8-13 Hz), as given by Eq. 2:

$$\mathrm{IAF} = \arg \max_{f \in [8,13]} P(f) \tag{2}$$

Using the estimated IAF, a subject-specific bandpass filter was constructed with a passband centered around the peak alpha frequency, as defined in Eq. 3:

$$[\mathrm{IAF} - 2,\ \mathrm{IAF} + 2]\ \mathrm{Hz} \tag{3}$$

Applying this filter to $x(t)$ yielded the alpha-band signal $X_\alpha(t)$, representing the dominant posterior alpha oscillation centered around the individual peak frequency.

3.3 Instantaneous phase and short-horizon prediction

The instantaneous phase of the filtered signal $X_\alpha(t)$ was estimated using the Hilbert transform to obtain its analytic signal Boashash (2002b;a):

$$z(t) = X_\alpha(t) + i\,\mathcal{H}\{X_\alpha(t)\} \tag{4}$$

where $\mathcal{H}\{\cdot\}$ in Eq. 4 denotes the Hilbert transform and i is the imaginary unit. The instantaneous phase was then computed from the analytic signal using Eq. 5:

$$\phi(t) = \arg\left(z(t)\right) \tag{5}$$

The estimated phase $\phi(t)$ was unwrapped prior to subsequent analysis. The instantaneous frequency $(f(t))$ was derived using the unwrapped phase $\phi(t)$:

$$f(t) = \frac{1}{2\pi} \frac{d\phi(t)}{dt} \tag{6}$$

Using the estimate from Eq. 6, the phase was locally extrapolated over a short temporal horizon Δ (in milliseconds) using Eq. 7. This corresponds to a local linear extrapolation of phase based on the instantaneous frequency. Importantly, this is not intended as a long-term forecasting model, but rather as a probe of short-horizon phase stability.

$$\hat{\phi}(t+\Delta) = \phi(t) + 2\pi f(t)\Delta \tag{7}$$

The prediction error was quantified using a circular error metric to account for the periodic nature of the phase:

$$e(t,\Delta) = \left| \angle \left(e^{i\left(\phi(t+\Delta) - \hat{\phi}(t+\Delta)\right)} \right) \right| \tag{8}$$

where $\angle(\cdot)$ in Eq. 8 denotes the phase angle, ensuring the error is computed on the unit circle and bounded within $[-\pi, \pi]$. The mean absolute prediction error over all time points was computed as:

$$E(\Delta) = \frac{1}{N_\Delta} \sum_t |e(t,\Delta)| \tag{9}$$

where N_Δ in Eq. 9 denotes the number of valid samples for which the prediction can be evaluated. The analysis was performed for multiple prediction horizons, specifically $\Delta = 50, 100, 150,$ and 200 ms, corresponding to 25, 50, 75, and 100 samples at a sampling frequency of 500 Hz.

3.4 Diffusion slope estimation

To quantify the temporal evolution of phase predictability, the mean error $E(\Delta)$ was modeled as a function of the prediction horizon Δ. In stochastic oscillator theory, the phase evolution of a noisy oscillator exhibits diffusion-like behavior, such that the variance of phase increments grows linearly with time Pikovsky et al. (1985):

$$\mathrm{Var}\big[\phi(t+\Delta) - \phi(t)\big] \propto D\,\Delta \tag{10}$$

where D is the phase diffusion coefficient in Eq. 10. Although the present study does not directly estimate phase variance, the growth of mean absolute phase prediction error with prediction horizon provides an empirical proxy for phase diffusion dynamics. Because phase estimation from EEG is affected by measurement noise and signal quality, the estimated slope should be interpreted as an effective phase predictability measure rather than a direct estimate of the physical diffusion coefficient. Motivated by this, the empirical error $E(\Delta)$ was modeled using a linear approximation over short horizons:

$$E(\Delta) \approx a + b\Delta \tag{11}$$

a, b in Eq. 11 denote the intercept and slope of error growth with respect to the prediction horizon. The larger values of b indicate faster loss of phase predictability over time. For each subject and experimental condition (Yaman, Puriya Dhanashree, Relaxation), the diffusion slopes were estimated by performing linear regression of $E(\Delta)$ against Δ. The detailed flowchart depicting the complete methodology is presented in Fig. 1.

The detailed methodology is summarized in Algorithm 1.

4 Results

4.1 Posterior alpha-band activity

To determine the presence of alpha-band activity in the posterior region prior to subsequent analysis, the power spectral density (PSD) of the averaged EEG signal $x(t)$ was computed. The mean PSD for all subjects and conditions (Yaman, Puriya Dhanashree, and Relaxation) is shown in Fig. 2. A clear peak is observed within the alpha frequency range ($8 - 13$ Hz) for all conditions, confirming the presence of posterior alpha activity. In addition, the alpha-band power appears comparable between the two music conditions (Yaman and Puriya Dhanashree), whereas the relaxation condition exhibits relatively lower power.

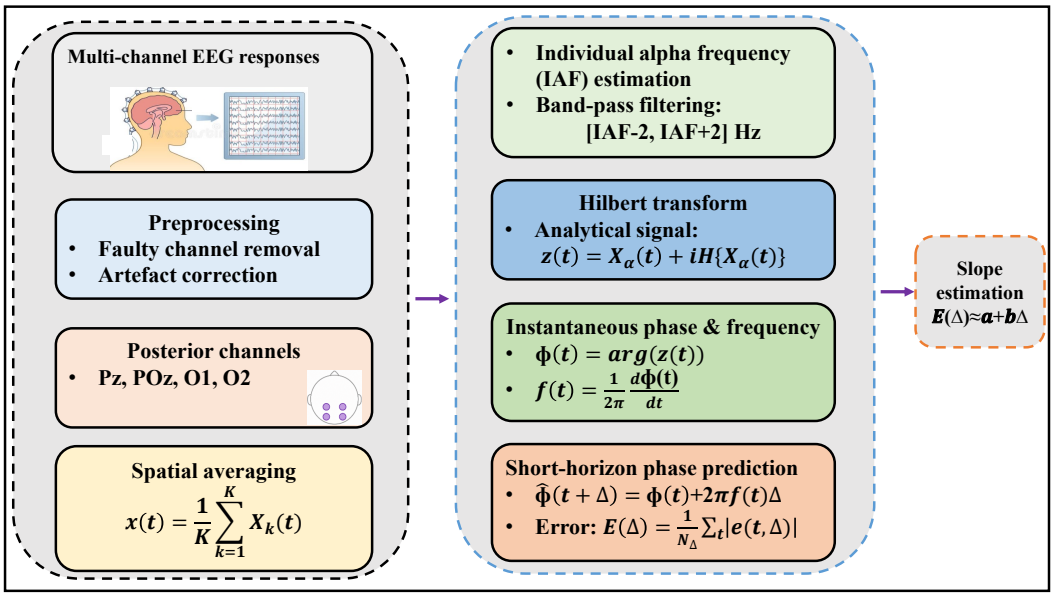


Figure 1: The pictorial representation of the proposed methodology showing the major steps involved: preprocessing, posterior channel selection, bandpass filtering, short-horizon phase prediction, and diffusion slope estimation.

Algorithm 1 Short-horizon phase prediction and diffusion slope estimation

Require: Multi-channel EEG signals $X_k(t)$ for each subject
Ensure: Diffusion slope b for each subject and condition
Select posterior channels: O1, O2, POz, Pz
Let K be the number of retained channels
Compute mean posterior signal: $x(t) = \frac{1}{K}\sum_{k=1}^{K} X_k(t)$
Estimate PSD $P(f)$ of $x(t)$ using Welch's method
Compute individual alpha frequency: $\text{IAF} = \arg\max_{f\in[8,13]} P(f)$
Apply bandpass filter $[\text{IAF}-2,\ \text{IAF}+2]$ Hz to obtain $X_\alpha(t)$
Compute analytic signal: $z(t) = X_\alpha(t) + i\,\mathcal{H}\{X_\alpha(t)\}$
Compute instantaneous phase: $\phi(t) = \arg(z(t))$
Unwrap $\phi(t)$
Estimate instantaneous frequency: $f(t) = \frac{1}{2\pi}\frac{d\phi(t)}{dt}$
for each prediction horizon $\Delta \in \{50, 100, 150, 200\}$ ms **do**
    Convert Δ to samples
    for each valid time index t **do**
        Compute phase extrapolation: $\hat{\phi}(t+\Delta) = \phi(t) + 2\pi f(t)\Delta$
        Compute circular error: $e(t,\Delta) = \left|\angle\left(e^{i(\phi(t+\Delta)-\hat{\phi}(t+\Delta))}\right)\right|$
    end for
    Compute mean error: $E(\Delta) = \frac{1}{N_\Delta}\sum_t |e(t,\Delta)|$
end for
Fit linear model: $E(\Delta) \approx a + b\Delta$
return diffusion slope b

4.2 Short-horizon phase prediction

To evaluate the short-horizon predictability of the alpha-band phase dynamics, the mean absolute phase prediction error was computed for a prediction horizon of $\Delta = 100$ ms. Both music conditions, Yaman (0.30 rad) and Puriya Dhanashree (0.32 rad), showed lower prediction errors compared to the relaxation (0.40 rad) condition. This suggests that listening to music is associated with a re-

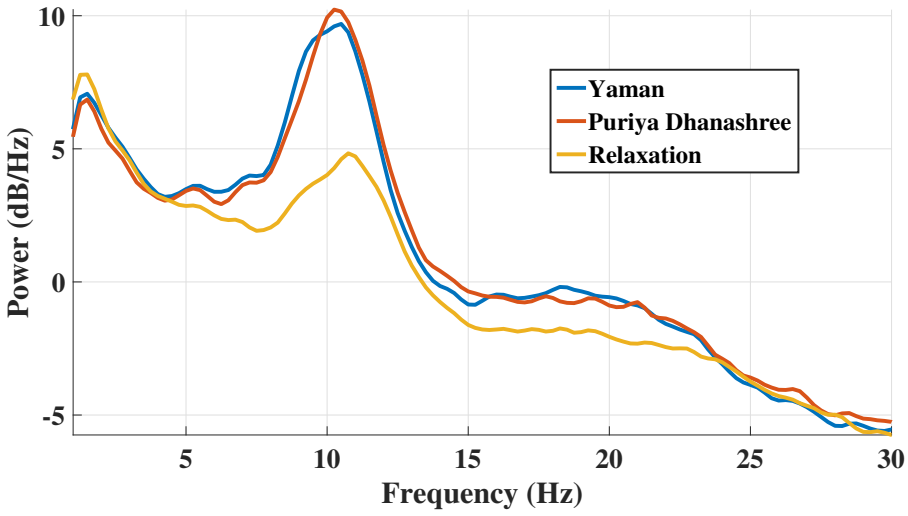


Figure 2: Mean posterior alpha-band power across all subjects for all conditions (Yaman, Puriya Dhanashree, and relaxation), showing a pronounced peak within the alpha-band frequency range (8-13 Hz).

duction in the local alpha-band phase prediction error relative to relaxation. The lower prediction error indicates the greater predictability of the short-horizon phase. This shows enhanced phase predictability during music conditions. Paired t-tests were performed between conditions, and effect sizes were quantified using Cohen's d. The resulting p-values and the effect sizes are presented in Table 2.

Table 2: Mean absolute phase prediction error across different conditions (Yaman, Puriya Dhanashree, and relaxation) for all the subjects. The error is for the horizon $\Delta = 100$ ms.

Condition	Mean error (rad)	Comparison	p-value	Effect size (d)
Yaman	0.30	Yaman vs Relaxation	0.0009	1.21
Puriya Dhanashree	0.32	Puriya Dhanashree vs Relaxation	0.0070	0.90
Relaxation	0.40	Yaman vs Puriya Dhanashree	0.3970	-

From Table 2, the paired t-test results indicate statistically significant differences between both music conditions and the relaxation condition (Yaman vs. Relaxation: $p = 0.0009$; Puriya Dhanashree vs. Relaxation: $p = 0.0070$). In contrast, no statistically significant difference was observed between the two music conditions. Furthermore, the effect size analysis revealed large effects for both music conditions when compared to relaxation, with Cohen's $d = 1.21$ for Yaman and $d = 0.90$ for Puriya Dhanashree. These values indicate a substantial reduction in phase prediction error during music listening relative to relaxation.

To examine the temporal dynamics of phase stability, we computed prediction errors across multiple horizons ($\Delta = 50, 100, 150, 200$ ms). The phase prediction errors with multiple prediction horizons are presented in Fig. 3. The mean prediction error increased monotonically with horizon across all conditions, consistent with stochastic diffusion-like behavior in neural oscillators. It is also observed that, the music conditions maintained lower errors relative to relaxation across all horizons. The mean absolute errors for all the conditions (Yaman, relaxation and Puriya Dhanashree) for different horizons are presented in Table 3. The table shows that the error is higher in the relaxation condition

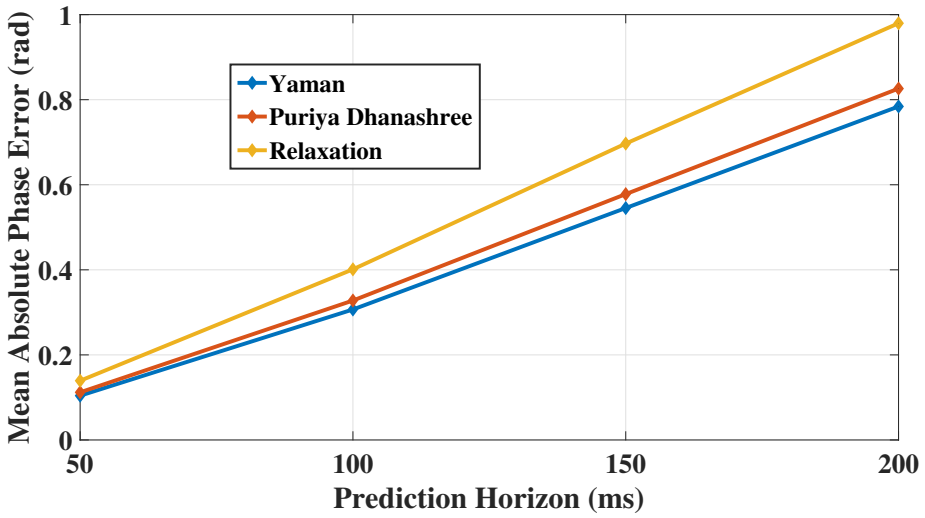


Figure 3: Mean absolute phase prediction error (rad) across prediction horizons ($\Delta = 50, 100, 150,$ and 200 ms) in the posterior region (O1, O2, POz, and Pz) for Yaman, Puriya Dhanashree, and relaxation conditions for all the subjects. The prediction error increases with horizon for all conditions.

compared to both musical conditions (Yaman and Puriya Dhanashree) for all the horizons. It is also observed that the mean absolute error is increasing linearly from a 50 ms horizon to a 200 ms horizon. This multi-horizon analysis provides evidence that the association between music listening and reduced phase predictability error is not limited to a single horizon. It extends across multiple horizons, reflecting a robust modulation of alpha-band dynamics.

Table 3: Mean absolute phase prediction error (rad) across multiple prediction horizons for all conditions and all the subjects.

Horizon (Δ in ms)	**Mean absolute phase error (rad)**		
	Yaman	**Puriya Dhanashree**	**Relaxation**
50	0.10	0.11	0.13
100	0.30	0.32	0.40
150	0.54	0.57	0.69
200	0.78	0.82	0.97

4.3 PHASE DIFFUSION SLOPES

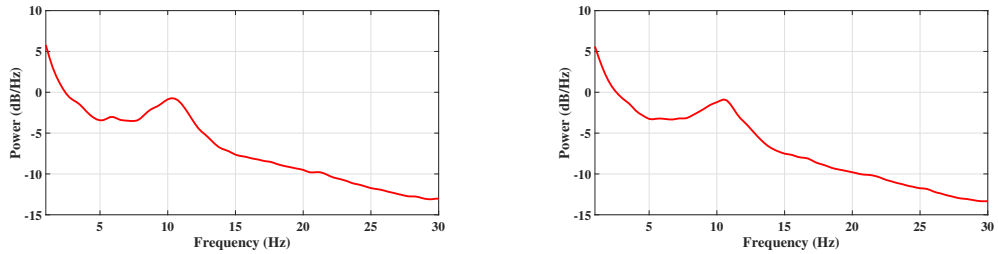
The relationship between mean absolute error and the short-horizons was modeled linearly using Eq. 11. The mean diffusion slopes for all the subjects and conditions (Yaman, Puriya Dhanashree, and Relaxation) for all the chosen horizons (50, 100,150,200 ms) were presented in Table 4. It was observed that the mean diffusion slopes were lower in both music conditions (Yaman: 0.0045; Puriya Dhanashree: 0.0047) compared to the relaxation condition (0.0056). It is also observed that the p-values from the paired t-test were statistically significant for both music conditions: Yaman vs Relaxation = 0.0008; Puriya Dhanashree vs Relaxation: p = 0.0050. No significant differences were observed between music conditions (p = 0.4237). Lower diffusion slopes indicate slower accumulation of short-horizon phase prediction error, suggesting greater temporal stability of alpha oscillations. This suggests that music listening is associated with differences in ongoing neural dynamics and temporal organization of oscillatory activity.

Table 4: Mean diffusion slopes obtained from the linear fit of phase prediction error as a function of prediction horizon for Yaman, Puriya Dhanashree, and relaxation conditions for all the subjects.

Condition	Diffusion slope	Comparison	p-value
Yaman	0.0045	Yaman vs Relaxation	0.0008
Puriya Dhanashree	0.0047	Puriya Dhanashree vs Relaxation	0.0050
Relaxation	0.0056	Yaman vs Puriya Dhanashree	0.4237

5 Implementation of the proposed framework on naturalistic music EEG dataset - tempo (NMED-T)

To evaluate the robustness of the proposed framework, we employed the Naturalistic Music EEG Dataset–Tempo (NMED-T) Losorelli et al. (2017a). The dataset contains EEG from 20 participants while they listened to 10 distinct songs. The EEG data were acquired using a 128-channel EEG cap at a sampling frequency of 1 kHz. During preprocessing, the data were downsampled to 125 Hz, and the clean data were aggregated across participants for each song. We selected the posterior channels from the 128 channels and performed the same analysis as we did on the ICM dataset. This dataset has no relaxation condition; we randomly selected songs 1 and 7 to apply the proposed methodology.



(a) Song 1 **(b)** Song 7

Figure 4: Mean posterior alpha-band power across all subjects for both songs 1 and 7 for the NMED-T dataset, showing a peak in the alpha-band (8–13 Hz).

The mean PSD plots for both songs across all 20 participants in the posterior region are shown in Fig. 4. This confirms the presence of alpha-band activity in the posterior region for this music dataset as well. Further, we compute the mean prediction error across all subjects for the horizon $\Delta = 100$ ms for both songs. The mean prediction error for song 1 is 0.474 rad and for song 7 is 0.477 rad. The mean absolute phase prediction errors (rad) for all four prediction horizons, averaged across all subjects and both songs, are presented in Table 5. As shown in the table, the prediction error increases progressively with the prediction horizon, from 50 ms to 200 ms. This trend is consistent with observations from the ICM dataset.

Table 5: Mean absolute phase prediction error (rad) for NMED-T dataset across multiple prediction horizons for all conditions and all the subjects.

Horizon (Δ in ms)	Mean absolute error (rad)	
	Song 1	Song 7
50	0.187	0.188
100	0.474	0.477
150	0.671	0.678
200	0.927	0.935

AI USE STATEMENT

In this work, ChatGPT was used solely as an assistive tool to improve English grammar, language clarity, and readability. All scientific content, including the ideas, methodology, analysis, and conclusions, was developed by the authors.

ETHICS STATEMENT

This study involved human participants and was conducted following institutional ethical guidelines. Informed consent was obtained from all participants before data collection.

REFERENCES

Yoshua Bengio and Yann LeCun. Scaling learning algorithms towards AI. In *Large Scale Kernel Machines*. MIT Press, 2007.

Boualem Boashash. Estimating and interpreting the instantaneous frequency of a signal. ii. algorithms and applications. *Proceedings of the IEEE*, 80(4):540–568, 2002a.

Boualem Boashash. Estimating and interpreting the instantaneous frequency of a signal. i. fundamentals. *Proceedings of the IEEE*, 80(4):520–538, 2002b.

György Buzsáki. *Rhythms of the Brain*. Oxford university press, 2006.

Mike X Cohen. *Analyzing neural time series data: theory and practice*. MIT press, 2014.

Gabriela Cruz, María Melcón, Leonardo Sutandi, J Matias Palva, Satu Palva, and Gregor Thut. Oscillatory brain activity in the canonical alpha-band conceals distinct mechanisms in attention. *The Journal of Neuroscience*, 45(1):e0918242024, 2025.

Arnaud Delorme and Scott Makeig. Eeglab: an open source toolbox for analysis of single-trial eeg dynamics including independent component analysis. *Journal of neuroscience methods*, 134(1): 9–21, 2004.

Bard Ermentrout and David M Terman. *Mathematical foundations of neuroscience*, volume 35. Springer, 2010.

John J Foxe and Adam C Snyder. The role of alpha-band brain oscillations as a sensory suppression mechanism during selective attention. *Frontiers in psychology*, 2:154, 2011.

Pascal Fries. A mechanism for cognitive dynamics: neuronal communication through neuronal coherence. *Trends in cognitive sciences*, 9(10):474–480, 2005.

Ian Goodfellow, Yoshua Bengio, Aaron Courville, and Yoshua Bengio. *Deep learning*, volume 1. MIT Press, 2016.

Thomas H Grandy, Markus Werkle-Bergner, Christian Chicherio, Martin Lövdén, Florian Schmiedek, and Ulman Lindenberger. Individual alpha peak frequency is related to latent factors of general cognitive abilities. *Neuroimage*, 79:10–18, 2013.

JASPER H. H. Ten-twenty electrode system of the international federation. *Electroencephalogr. Clin. Neurophysiol.*, 10:371–375, 1958.

Uri Hasson, Yuval Nir, Ifat Levy, Galit Fuhrmann, and Rafael Malach. Intersubject synchronization of cortical activity during natural vision. *science*, 303(5664):1634–1640, 2004.

Doli Hazarika, Srihari Madhavan, and Cota Navin Gupta. Cameraeeg: Synchronous recording of electroencephalogram and video data for neuroergonomics applications. *Engineering Proceedings*, 55(1):46, 2023.

Geoffrey E. Hinton, Simon Osindero, and Yee Whye Teh. A fast learning algorithm for deep belief nets. *Neural Computation*, 18:1527–1554, 2006.

Ole Jensen and Ali Mazaheri. Shaping functional architecture by oscillatory alpha activity: gating by inhibition. *Frontiers in human neuroscience*, 4:186, 2010.

Blair Kaneshiro, Duc T Nguyen, Anthony M Norcia, Jacek P Dmochowski, and Jonathan Berger. Inter-subject correlation of electroencephalographic and behavioural responses reflects time-varying engagement with natural music. *European Journal of Neuroscience*, 59(12):3162–3183, 2024.

Wolfgang Klimesch. Eeg alpha and theta oscillations reflect cognitive and memory performance: a review and analysis. *Brain research reviews*, 29(2-3):169–195, 1999.

Wolfgang Klimesch, Michael Doppelmayr, Th Pachinger, and Barbara Ripper. Brain oscillations and human memory: Eeg correlates in the upper alpha and theta band. *Neuroscience letters*, 238 (1-2):9–12, 1997.

Wolfgang Klimesch, Paul Sauseng, and Simon Hanslmayr. Eeg alpha oscillations: the inhibition–timing hypothesis. *Brain research reviews*, 53(1):63–88, 2007.

Yoshiki Kuramoto. Chemical turbulence. In *Chemical oscillations, waves, and turbulence*, pp. 111–140. Springer, 1984.

Jean-Philippe Lachaux, Eugenio Rodriguez, Jacques Martinerie, and Francisco J Varela. Measuring phase synchrony in brain signals. *Human brain mapping*, 8(4):194–208, 1999.

Edward W Large, Jorge A Herrera, and Marc J Velasco. Neural networks for beat perception in musical rhythm. *Frontiers in systems neuroscience*, 9:159, 2015.

Yuan-Pin Lin, Chi-Hong Wang, Tzyy-Ping Jung, Tien-Lin Wu, Shyh-Kang Jeng, Jeng-Ren Duann, and Jyh-Horng Chen. Eeg-based emotion recognition in music listening. *IEEE Transactions on Biomedical Engineering*, 57(7):1798–1806, 2010.

Steven Losorelli, Duc T Nguyen, Jacek P Dmochowski, and Blair Kaneshiro. Naturalistic music eeg dataset—tempo (nmed-t). *Stanford Digital Repository. Retrieved January*, 15:2019, 2017a.

Steven Losorelli, Duc T Nguyen, Jacek P Dmochowski, and Blair Kaneshiro. Nmed-t: A tempo-focused dataset of cortical and behavioral responses to naturalistic music. In *ISMIR*, volume 3, pp. 5, 2017b.

Alireza Malekmohammadi, Stefan K Ehrlich, Josef P Rauschecker, and Gordon Cheng. Listening to familiar music induces continuous inhibition of alpha and low-beta power. *Journal of Neurophysiology*, 129(6):1344–1358, 2023.

Dante Mantini, Mauro G Perrucci, Cosimo Del Gratta, Gian L Romani, and Maurizio Corbetta. Electrophysiological signatures of resting state networks in the human brain. *Proceedings of the National Academy of Sciences*, 104(32):13170–13175, 2007.

Kana Mizokuchi, Toshihisa Tanaka, Takashi G Sato, and Yoshifumi Shiraki. Alpha band modulation caused by selective attention to music enables eeg classification. *Cognitive Neurodynamics*, 18 (3):1005–1020, 2024.

Hiroya Nakao. Phase reduction approach to synchronisation of nonlinear oscillators. *Contemporary physics*, 57(2):188–214, 2016.

Ernst Niedermeyer and FH Lopes da Silva. *Electroencephalography: basic principles, clinical applications, and related fields*. Lippincott Williams & Wilkins, 2005.

Sylvie Nozaradan, Isabelle Peretz, Marcus Missal, and André Mouraux. Tagging the neuronal entrainment to beat and meter. *Journal of Neuroscience*, 31(28):10234–10240, 2011.

Paul L Nunez and Ramesh Srinivasan. *Electric fields of the brain: the neurophysics of EEG*. Oxford university press, 2006.

Satu Palva and J Matias Palva. New vistas for α-frequency band oscillations. *Trends in neurosciences*, 30(4):150–158, 2007.

Satyam Panda, Dasari Shivakumar, Yagnyaseni Majumder, Cota Navin Gupta, and Budhaditya Hazra. Real-time measures for brain activity detection to live indian classical music stimulus. In *2023 IEEE 20th India Council International Conference (INDICON)*, pp. 179–185. IEEE, 2023.

Satyam Panda, Dasari Shivakumar, Yagnyaseni Majumder, Cota Navin Gupta, and Budhaditya Hazra. Real-time dynamic analysis of eeg response for live indian classical vocal stimulus with therapeutic indications. *Smart Health*, pp. 100461, 2024.

David Pascucci, Maëlan Q Menétrey, Edoardo Passarotto, Junlian Luo, Matilde Paramento, and Maria Rubega. Eeg brain waves and alpha rhythms: Past, current and future direction. *Neuroscience & Biobehavioral Reviews*, pp. 106288, 2025.

Arkady Pikovsky, Michael Rosenblum, Jürgen Kurths, and A Synchronization. *A universal concept in nonlinear sciences*. Cambridge University Press, Princeton, 1985.

Arkady Pikovsky, Michael Rosenblum, and Jürgen Kurths. *Synchronization: A universal concept in nonlinear sciences*. Cambridge University Press, 2003.

Daniela Sammler et al. Music and emotion: electrophysiological correlates. *Cerebral Cortex*, 17 (11):2603–2611, 2007.

Dasari Shivakumar, Cota Navin Gupta, and Budhaditya Hazra. Geometry-based visualization of brain activity in live music. In *2026 IEEE Guwahati Subsection Conference (GCON)*, pp. 1–6. IEEE, 2026a.

Dasari Shivakumar, Cota Navin Gupta, and Budhaditya Hazra. Long-range correlations in alpha-band of electroencephalogram: a nonlinear embedding and detrended fluctuation analysis. *Frontiers in Neuroinformatics*, 20:1823408, 2026b.

Markus Siegel, Tobias H Donner, and Andreas K Engel. Spectral fingerprints of large-scale neuronal interactions. *Nature Reviews Neuroscience*, 13(2):121–134, 2012.

Ben Somers, Tom Francart, and Alexander Bertrand. A generic eeg artifact removal algorithm based on the multi-channel wiener filter. *Journal of neural engineering*, 15(3):036007, 2018.

Saurabh Sonkusare, Michael Breakspear, and Christine Guo. Naturalistic stimuli in neuroscience: critically acclaimed. *Trends in cognitive sciences*, 23(8):699–714, 2019.

Connor Spiech, Anne Danielsen, Bruno Laeng, and Tor Endestad. Oscillatory attention in groove. *cortex*, 174:137–148, 2024.

Parker Tichko, Nicole Page, Ji Chul Kim, Edward W Large, and Psyche Loui. Neural entrainment to musical pulse in naturalistic music is preserved in aging: Implications for music-based interventions. *Brain Sciences*, 12(12):1676, 2022.

Arthur T Winfree. *The geometry of biological time*, volume 2. Springer, 1980.